

Chabazite and dolomite formation in a dolocrete profile an example  
of complex alkaline paragenesis in Lanzarote, Canary Islands

Ana M. Alonso-Zarza\* <sup>1,2</sup>, Leticia Bustamante<sup>1</sup>, Pedro Huerta<sup>3</sup>, Álvaro  
Rodríguez-Berriguete<sup>1,2</sup>, María José Huertas<sup>1</sup>

<sup>1</sup> *Departamento de Petrología y Geoquímica, Fac. CC. Geológicas, Universidad Complutense de  
Madrid, C/ José Antonio Novais, 2, 28040 Madrid, Spain. [alonsoza@ucm.es](mailto:alonsoza@ucm.es)*

<sup>2</sup> *Instituto de Geociencias, IGEO (CSIC, UCM). C/ José Antonio Novais, 2, 28040 Madrid, Spain.*

<sup>3</sup> *Departamento de Geología, Escuela Politécnica Superior de Ávila, Universidad de Salamanca,  
Avd/ Hornos Caleros, 50, 05003 Ávila, Spain.*

\*Corresponding autor: Ana M<sup>a</sup> Alonso-Zarza. phone (34) 913944915

**Key-words:** Dolocrete, zeolites, groundwater, pedogenic, basalts, Canary  
Islands.

## ABSTRACT

This paper studies the weathering and soil formation processes operating on detrital sediments containing alkaline volcanic rock fragments of the Mirador del Río dolocrete profile. The profile consists of a lower horizon of re-mobilised weathered basalts, an intermediate red sandy mudstones horizon with irregular carbonate layers and a topmost horizon of amalgamated carbonate layers with root traces. Formation occurred in arid to semiarid climates, giving place to a complex mineralogical association, including Mg-carbonates and chabazite, rarely described in cal/dolocretes profiles. Initial vadose weathering processes occurred in the basalts and in directly overlying detrital sediments, producing (Stage 1) red-smectites and dolomicrite. Dominant phreatic (Stage 2) conditions allowed precipitation of coarse-zoned dolomite and chabazite filling porosities. In Stages 3 and 4, mostly pedogenic, biogenic processes played an important role in dolomite and calcite accumulation in the profile. Overall evolution of the profile and its mineralogical association involved initial processes dominated by alteration of host rock, to provide silica and Mg-rich alkaline waters, suitable for chabazite and dolomite formation, without a previous carbonate phase. Dolomite formed both abiogenically and biogenically, but without a previous carbonate precursor and in the absence of evaporites. Dominance of calcite towards the profile top is the result of Mg/Ca decrease in the interstitial meteoric waters due to decreased supply of Mg from weathering, and increased supply of Ca in eolian dust. Meteoric origin of the water is confirmed by C and O isotope values, which also indicate lack of deep sourced CO<sub>2</sub>. The dolocrete

studied and its complex mineral association reveal the complex interactions that occur at surface during weathering and pedogenesis of basalt-sourced rocks.

## 1. Introduction

Calcretes and dolocretes, commonly described in sedimentary basins developed on sedimentary host rocks (Goudie, 1973; Esteban and Klappa, 1983; Alonso-Zarza and Wright, 2010), do also form on metamorphic and igneous (Chiquet et al., 1999, 2000; Capo et al., 2000; Kadir, et al., 2010) host rocks. Of special interest is the accumulation of carbonate minerals on weathering profiles/soils containing basaltic rocks, as weathering of these rocks under alkaline conditions gives place to complex mineralogy including Mg-Ca-rich silicate minerals, such as various types of zeolites, smectites (Whipkey et al., 2002) or talc-like minerals. Interpretation of the processes involved in the formation of this association is important for several reasons: 1) dolomite occurring in this type of soils is commonly ordered and stoichiometric (Capo et al., 2000; Whipkey et al., 2002), uncommon in recently formed dolomites; 2) South Atlantic reservoirs of Brazil and Angola seem to be contained in rocks formed by these minerals (Wright and Barnett, 2015); 3) a similar association seems to be present in some areas of Mars, thus indicating the presence of liquid water on the Martian surface, and perhaps microbial activity (Brown et al., 2010; Sutter et al., 2012); and 4), as formation of carbonates on and within weathered basalts requires CO<sub>2</sub>, these carbonates might become useful as CO<sub>2</sub> sequestration sinks (Gysi and Stefánsson, 2012).

The volcanic Canary Islands show a broad development of pedogenic calcretes, especially in the more arid eastern-most Islands (Alonso-Zarza and Silva, 2002; Huerta et al., 2015). These calcretes, mostly composed of calcite, were supplied calcium from aeolian dust (Huerta et al., 2015). However little is known of the interaction of pedogenic-versus groundwater-accumulation of carbonates within weathered volcanic rocks, or in detrital deposits containing mostly volcanic fragments. In this paper we present the study of a calcrete/dolocrete profile that contains a typically alkaline mineral association including calcite, dolomite, smectites and chabazite (zeolite), developed in this type of rocks. Our aim is to discuss the mechanisms and controls operating in the formation of this mineral association within cal-dolocrete profiles hosted on volcanic-sourced surficial deposits, to better understand the origin of dolomite in soils. In addition, our study may serve as a near-natural analogue for a better understanding of CO<sub>2</sub> sequestration in mafic rocks, or to shed light on processes involved in the formation of this alkaline association in Mars.

## **2. Geological setting**

The Canary Islands, a volcanic archipelago comprising seven main islands and several islets, situated close to the African coast (Fig.1), lies on oceanic African crust of early Jurassic age (Verhoef et al., 1991; Ancochea et al., 2004). The age of island emergence decreases from E to W. Younger islands, La Palma and El Hierro, are about 1.2 million years old, while Lanzarote and Fuerteventura, the eastern-most, are the oldest islands, 15 and 23 Ma respectively (Balogh et al., 1999; Van den Bogaard, 2013). In Lanzarote

there are two main volcanic cycles (Balcells et al., 2004): during the first cycle (Upper Miocene to Pliocene), volcanic shields (Ajaches and Famara) formed (Coello et al., 1992). These volcanic shields were coated by recent volcanism (Fúster et al., 1968). In the Famara Massif, the last eruption was the Corona volcano,  $21000 \pm 6500$  years ago (Carracedo et al., 2003).

Lanzarote Island, in a senile evolutive stage dominated by erosive and sedimentary processes (Carracedo, 2011), contains quaternary marine terraces, aeolian deposits and calcretes (Zazo et al., 2002; Meco, 2008). Calcretes were formed after the Pliocene in relatively less-arid interglacial periods (Alonso-Zarza and Silva, 2002; Genise et al., 2013). Due to their location near Africa, all the Canary islands are regularly affected by aeolian dust (Goudie and Middleton, 2006; Menéndez et al., 2007; Scheuven et al., 2013) from the northern part of the continent, the Sahara and Sahel regions (Laurent et al., 2008; Muhs et al., 2010). This dust was the main source of calcium and carbonate for calcrete formation in the eastern-most Canary Islands. In addition some areas of the islands marine bioclasts fragments transported mainly by wind periods were also an additional Ca-source for calcrete development (Meco, 2008; Criado et al., 2012; Huerta et al., 2015).

The Mirador del Río profile, from the northernmost part of Lanzarote, on the slope of Famara cliff, is located in the homonym massif. The outcrop studied is about 470 m above mean sea level ( $29^{\circ} 12' 46.0''$  N,  $13^{\circ} 28' 58.3''$  W) (Fig.1). The cliff is a retrograded scarp from a giant gravitational collapse scarp (Carracedo et al., 2002) of part of the volcano, 10.2 - 3.8 Ma (Coello et al., 1992). The Famara Massif consists of a thick tabular succession of basaltic lava flows (1 to 2 m thick) with interbedded pyroclasts falls of the same geochemical

compositions, more than 7% of MgO. These volcanic very dark rocks, contain olivine and augite phenocrysts, altered to iddingsite, within a fine vitreous groundmass. Vacuoles within the basalts are partially filled by carbonates and zeolites (Balcells et al., 2004).

Basaltic lava flows are discordantly overlain by upper Pleistocene detrital deposits consisting of 25 m of angular and heterometric volcanic fragments within a red clay matrix (Balcells et al., 2004). These poorly stratified beds were supplied with clasts and red matrix from nearby weathered basalts. Textural and compositional features indicate a minimum transport. The studied Mirador del Río profile developed within these detrital beds.

### 3. Methods

Seven representative samples were taken from the Mirador del Río profile. Thin sections were made for petrographical analysis and characterization of the different microtextures was done by transmission-light microscopy. Due to fragility, samples were embedded in EPOXY resin, in a vacuum system.

Bulk-rock mineralogy was studied with a Philips PW-1710 X-Ray diffraction (XRD) system, operating at 40kV and 30 mA, under monochromatic CuK $\alpha$  radiation. Semi-quantitative analyses were performed using EVA software by Bruker. Mineralogical characterization of clay minerals was carried out on oriented aggregate samples using oriented air-dried slides that were ethylene glycol solvated and heated to 550°C (Brindley, 1961). Degree of dolomite ordering was determined by X-ray diffraction according to Goldsmith and Graf

(1958) procedures, and Hardy and Tucker (1988). SEM studies were performed with a scanning electron microscope, model JEOL JSM-820, equipped with an energy dispersive X-ray analyzer (EDX) of the CAI of geological techniques of Complutense University of Madrid (Spain).

Chemical microanalyses of the main minerals for different elements, were made by wavelength dispersive electron probe microanalyzer (WDS-EPMA), model JEOL JXA 89000, in the Electronic Microscopy Center Luis Brú of Complutense University of Madrid. These analyses were performed on gold-coated, polished sections.

The  $\delta^{13}\text{C}$  and  $\delta^{18}\text{O}$  values for dolomite and calcite from six samples were determined at the Scientific and Technical Services of Barcelona University (Spain). Analyses were carried out on powdered samples. To analyze calcite and dolomite, samples were attacked with hydrochloric acid diluted to 10% by measuring isotopic ratios for calcite after one minute attack. Twenty minutes later, samples were washed with distilled water, filtered and oven-dried, and values for dolomite were determined.  $\text{CO}_2$  was extracted using a Thermo Finnigan Carbonate Kiel Device III isotopic analyzer, with a Thermo Finnigan MAT-252 spectrometer, according to the McCrea (1950) method. Values obtained were corrected using the NBS-19 standard value and referred to VPDB standard.

#### **4. The Mirador del Río profile**

##### *4.1. Macromorphology of the profile*

Poorly stratified detrital deposits of the Famara Cliff contain a 2.4 m thick bed (Figs 2, 3A), formed by red-orange mudstones with intercalated irregular carbonate layers. Lateral continuity of the bed is about 40 m, as it pinches out to the SW and towards the NE, directly overlying weathered basalts. The bed constitutes the Mirador del Río profile, formed by three horizons (Fig. 2).

The lower horizon, the transition with volcanic rock, is 0.2-0.4 m thick, composed of weathered basalts partially remobilised, and including large, angular and poorly-sorted basalt fragments within a silty matrix.

The intermediate, brown-red horizon, 1.5-1.9 m thick, is composed of sandy mudstones with oxidized gravel-sized clasts of basalts with interbedded carbonate layers (Fig. 3B). Mudstones show irregular mm-wide cracks partially filled with white cement (Fig. 3C). The irregular horizontal carbonate layers (2-10 cm thick), confer a platy structure to the horizon. These layers, more separated at the base of the horizon, tend to coalesce and amalgamate towards the top. The carbonate is mostly dolomite at the base of the horizon, but the amount of calcite increases towards the top (Fig. 2).

The upper horizon consists of amalgamated, mostly calcite, carbonate layers with few inter-bedded red mudstones. Root traces confer a diffuse prismatic structure to the horizon, 0.30 m thick, in gradual contact with the lower horizon, overlain at the top by red silts.

#### *4.2. Mineralogy and Petrology*

Thin sections show that samples are composed of a fine groundmatrix which includes micrite, dolomicrite and clays (Figs. 4, 5). In the lower horizon



and in the and less carbonate layers of the intermediate horizon coarse detrital clasts (fragments of volcanic rocks, olivines, fragments of coarse crystalline dolomite and chabazite) are irregularly distributed within the groundmatrix, which is cut by empty or dolomite and/or chabazite filled circum-granular and planar cracks (Fig. 4A, 5A). The carbonate layers either dolomite (Fig. 4B, 5B) or calcite (Fig. 4C, 5C) include coated grains, irregular laminations and alveolar septal structures, but lack chabazite or dolomite filled cracks. Mineralogy of the profile is complex, including a wide variety of components (Table 1) inherited from both the host rock and minerals formed within the soil profile.

1.- Fragments of volcanic rocks and volcanic minerals have porphyritic texture with olivine and augite phenocrysts included in a groundmass with opaques and glass. Some vacuoles contain chabazite; fragments are corroded, and their size may reach several mm. Olivine and augite occur within volcanic fragments and also as individual grains about 0.5 to 1 mm across, embedded in a carbonate-clayly matrix (Fig. 6A). Olivine is altered to iddingsite, a red-brown mass formed by saponite, goethite (Eggletton, 1984) and other clay minerals. Augite is altered to serpentine, uralite and chlorite, but less than is the olivine.

2.- Phyllosilicates occur as a dark, cracked groundmass mixed with dolomicrite, as relics within carbonate layers and as coatings on any silicate component of the profile (Fig. 6B). XRD studies indicate that they are mostly smectites, which is consistent with SEM observations (Fig. 6C).

3.- Chabazite is a zeolite which may contain different amounts of Na, K, Ca or Mg. Chabazites from the study profile are rich in Na (Table 1). In thin sections they appear as fibrous-radial or petaloid-like spherulites or more rarely as crystalline euhedral to subeuhedral equant mosaics (Fig. 6D-H). Fibrous-radial spherulites are about 0.5 mm in diameter. Petaloid spherulites are smaller (0.2 mm), composed of 6-10 triangular crystals. Chabazite occurs as: 1) detrital fragments; 2) cements partially or totally filling vacuoles or fractures within volcanic fragments; and 3) cements filling cracks within the micrite carbonate matrix or around detrital grains. In many cases, especially cases 1 and 3, chabazite is partially replaced by dolomite (Fig. 6G, H).

4.- Dolomite is the only carbonate mineral in the lower part of the profile, but is also present in the upper part, together with calcite. It is either coarse crystalline or dolomicrite. Coarse crystalline dolomite appears as: 1) cements filling cracks, within the dolomicrite or micrite matrix or on weathered detrital grains, commonly distributed all throughout the pore or coating all the surface of specific grains (Figs. 4A, 7A), 2) partially replacing chabazite (Fig. 6G, H), 3) as detrital etched fragments, up to 2 mm across (Fig. 7B, C). This coarse dolomite is zoned, as clear dolomite bands are interrupted by dark-cloudy ones. Dolomicrite occurs as: 1) homogeneous or peloidal matrix, in cases replacing and corroding detrital grains (Figs 4B, 7C), 2) irregular and thin coatings on detrital grains (Fig. 7D), and commonly alternating with red clays, 3) micritic filaments (Fig. 7E), 4) forming irregular laminar structures (mm-thick) in which micrite alternates with irregular empty cracks. Some needle-like fibre crystals

also occur within dolomicrite (Fig. 7F). Very commonly dolomicrite is found coating or overlying dolomite cements or chabazite (Fig. 7E, F).

Dolomite, having superstructure peaks, lends itself to calculation of the degree of order (Goldsmith and Graf, 1958), which varies between 0.46 and 0.94 (Table 1). Samples with a higher order degree, in the lower part of the profile, has coarse dolomite more commonly than dolomicrite. The amount  $\text{CO}_3\text{Mg}$  varies between 40 and 44%, whereas  $\text{CO}_3\text{Ca}$  varies between 55 and 59%, indicative of a Ca-rich dolomite.

5.- Calcite, mostly micrite and rarely microspar, occurs mostly in the upper part of the profile. Calcite micrite occurs with an arrangement similar to that of dolomicrite, but micritic filaments and/or alveolar septal structures are more common (Fig. 7G, H). No features indicative of dedolomitization were found. XRD and microprobe analyses indicate that calcite is HMC with a mean  $\text{CO}_3\text{Mg}$  content of 9%.

#### 4.3. Isotope Geochemistry

Mean  $\delta^{13}\text{C}$  values are -8.90‰VPDV for calcite and -8.40 ‰VPDV for dolomite. Calcite has mean  $\delta^{18}\text{O}$  ‰VPDV values of -1.86 and dolomite of 0.54. Although the number of samples is limited, carbon values do not differ greatly between the calcite and dolomite of the same sample, whereas oxygen values are about 1‰ heavier in dolomite (Fig. 8). Oxygen values are in the range of other calcretes from Lanzarote and Fuerteventura islands (Huerta et al., 2015), whereas carbon values are, in general, lighter.  $^{87}\text{Sr}/^{86}\text{Sr}$  (0.7078 to 0.7081)

values are very similar to those obtained by Huerta et al., (2015) in calcretes developed on basaltic host rocks.

## **5. Discussion**

### *5.1. Mineral formation*

The complex mineralogy of this profile, specially the presence of chabazite, differentiates it from other calcrete profiles described in the eastern-most Canary Islands (Genise et al., 2013; Huerta et al., 2015), and also from most calcrete-dolocrete profiles in which chabazite is uncommon. Chabazite is common in volcanic settings either as a hydrothermal or weathering product (Robert et al., 1988). Very probably chabazite infills of some vacuoles of volcanic fragments occurred during hydrothermal alteration of basalts (Pérez-Torrado et al., 1995; Pérez-Guerrero et al., 1997; Robert, 2001). On the contrary, chabazite recognized in cracks formed during weathering caused by percolation of meteoric waters through porous volcanic material, as described by Gottardi (1989). Under semiarid to arid climates, evapotranspiration may produce alkaline conditions suitable for chabazite (and other zeolites) precipitation in soils (Hay and Sheppard, 2001), together with other zeolites and carbonates as described also in Olduvai Gorge (Tanzania) (Ashley and Driese, 2000). Chabazite precipitation is favoured by the presence of inherited chabazite in soils (Ming and Boettinger, 2001) as in this study case, where the coarse size of crystals and its presence mostly in cracks point to formation under phreatic conditions, either as cement or replacement of dolomite.

The two types of dolomite reflect different conditions, but in both cases dolomite formed in the absence of a previous carbonate precursor, as also described in soils of non-volcanic areas (Spötl and Wright, 1992; Casado et al., 2014). Coarse, zoned dolomite formed mostly as phreatic cements, as indicated by its symmetric arrangement and zoning around voids, and by the absence of any pedogenic features. Similar groundwater dolocretes, with dolomite filling different types of cavities, have also been described in karst settings (Khalaf, 1990; Khalaf and Abdullah, 2013), where dolomite was also considered a precipitate that did not replace any previous mineral. In fluvial groundwater dolocretes, dolomite saturation of groundwater is driven by the early precipitation of calcite, which caused an increase of Mg concentration (Spötl and Wright, 1992). However, this mechanism is excluded from the Mirador del Río profile, as there is neither previous calcite precursor nor the expectation of lateral chemical evolution of groundwaters. In our case, weathering of basaltic rocks or of their fragments produced Mg-rich solutions favoring dolomite formation, mostly as cement but also locally replacing chabazite (Podwojewski, 1995; Capo et al., 2000; Whipkey et al., 2002; Whipkey and Hayob, 2008). The generally arid to semi-arid climate, as that prevailing in the Canaries, could cause variations in the degree of saturation of groundwater, enabling the formation of zoned dolomite. Cloudy zones are probably partially dissolved dolomite, and the clear ones stable, undissolved dolomites (Khalaf and Abdullah, 2013), similarly to that described in cave aragonites, where micritization by partial dissolution produced dark, clouded bands (Martín-García et al., 2014).

Dolomicrite replacement of the soil matrix, grains with dolomite coatings, dolomicrite filaments and peloidal dolomicrite probably formed under vadose conditions and under some biogenic control, as also indicated by needle-like crystals and alveolar septal structures (Callot et al., 1985; Phillips and Self, 1987; Verrecchia and Verrecchia, 1994; Bajnóczi and Kovács-Kis, 2006; Cailleau et al., 2009). Very commonly these mostly fungal structures, interpreted as biogenic, are formed by calcite, aragonite or calcium oxalates, but rarely by dolomite. Some exceptions are various dolomite paleosols and marginal lacustrine deposits from the Madrid Basin, where dolomite occurs in clear association with roots, either mycorrhizae or otherwise (Sanz-Montero and Rodriguez-Aranda, 2012, Casado et al., 2014). Although the exact mechanism of dolomite formation is unknown, it would seem that both biogenic and abiogenic processes controlled dolomite formation in those alkaline vadose environments (Casado et al., 2014). Of additional interest is the need for nutrients of roots and associated microorganisms, with their associated acids promoting silicate weathering, favoring release of K, Mg, Ca and Fe (Calvaruso et al., 2006), also possibly favoring carbonate formation in soil (Sanz-Montero et al., 2009). Variation in the degree of order of dolomite probably is a reflection of the two different types of dolomite, but all have superstructure peaks and so are ordered dolomites. These ordered dolomites are common in soils developed in basalts (Capo et al., 2000) or Mg-rich clays (Casado et al., 2014), probably as a result of the relatively high Mg/Ca ratio in the pedogenic environment, which favors the incorporation of Mg into the dolomite structure.

The fact that micrite calcite postdates dolomite and has its same textures, points to the interplay of biogenic and non-biogenic processes, but

also indicates fresher waters with lower Mg/Ca ratios. Such change could be due to: 1) decreased supply of magnesium from groundwater, 2) dominance of pedogenic versus phreatic conditions, and 3) aeolian dust supply of Ca to the top of the profile (Huerta et al., 2015), as also confirmed by Sr isotope values. In this last stage of evolution of the profile roots played in calcite precipitation.

Carbon and oxygen data in the range of most pedogenic and groundwater calcretes (Spölt and Wright, 1992; Williams and Krause, 1998); confirm the either phreatic or vadose meteoric origin of the water, Dolomite shows higher oxygen values than calcite due to the fractionation effect (O'Neil and Epstein, 1966). Relatively higher oxygen values are an indication of the heavier values of rain water in the eastern-most Canary Islands (Yanes et al., 2008), as also seen in thick laminar calcrete profiles from Lanzarote and Fuerteventura (Huerta et al., 2015). Negative  $\delta^{13}\text{C}$  values confirm the meteoric origin of the water, precluding the influence of deep-sourced  $\text{CO}_2$ . The later would have produced positive or only slightly negative carbon values, as of those found in travertines from nearby Gran Canaria Island (Rodríguez-Berriguete et al., 2012; Camuera et al., 2014).

## *5.2. Profile formation*

The Mirador del Rio profile developed on weathered basalts and sandy mudstones directly overlying basalts. In the lower part of the profile it is difficult to distinguish “in situ” weathered basalts from detrital sandy mudstones. Clearer evidence comes from the presence of detrital grains of both chabazite and dolomite, which suggests the reworking of previously weathered basalts.

Weathering of detrital sandy mudstones produced red clays (smectites) that constitute, together with the dolomicrite, the matrix of an incipient paleosoil (Stage 1, Fig. 9). Formation of smectites was mainly due to the transformation of ferromagnesian minerals (Eggerton et al., 1987) such as olivine or augite. In addition, the presence of clay-cutans also points to illuvial processes within the profile (Wilson, 1999).

Dolomite precipitation as coarse crystals filling voids suggests a stage (Stage 2) of profile formation under groundwater conditions similar to some karst-related dolocretes (Khalaf and Abdullah, 2013). The magnesium required came from the weathering of basaltic rocks and basaltic components of the profile host rocks, which also supplied the cations required to form chabazite. Both weathering and precipitation of chabazite and dolomite occurred under seasonally contrasted arid to semi-arid climates, allowing the formation of zoned dolomite. Variable humidity conditions also could cause differences in pH or the supply of silica, Mg, or Na, favoring replacement of chabazite by dolomite, under alkaline, non-evaporite conditions. This context is somehow different from that commonly described for groundwater calcretes or dolocretes, as they seem to be linked to the presence of evaporite bodies (Arakel, 1986, 1991; Spölt and Wright, 1992; Colson and Cojan, 1996; Jutras et al. 2007), where dolomite formed as the result of evaporation and evapotranspiration which caused the down-dip increase of Mg/Ca ratio of groundwater due to previous calcite precipitation within sediments. Both the morphology of the profile and its geochemistry point to formation in meteoric groundwaters, with no influence of evaporites. In addition, detrital fragments of coarse zoned dolomite in various levels within the profile indicate surface reworking of older profiles.



Formation of dolomicrite (St 3) and the dominance of calcite (St 4) in the upper part of the profile suggest a change from dominant phreatic to vadose-pedogenic conditions. In these stages (Fig. 9), biogenic processes played an important role in accumulation of carbonate within the profile, with root mats contributing to the formation of the carbonate layers interbedded with the sandy mudstones as described in other rootcretes (Alonso-Zarza and Jones, 2007; Meléndez et al., 2011; Bustillo et al., 2013). Transition from dolomite to calcite is an indication of the decrease of Mg supply from weathering, as well as an increase of Ca supplied by eolian dust (Stage 4).

Composition of host rock (alkaline basaltic-like detritals) and arid to semiarid climatic conditions of Lanzarote, determined the formation of an alkaline mineral association under both phreatic and vadose (pedogenic) conditions. Study of the mineral association of these profiles has additional implications such as: 1) similar associations have recently been found in the surface of Mars (Ming et al., 2008; Sutter et al., 2012), so study of these profiles could provide clues to the understanding of environmental and geochemical conditions prevailing there; and 2), presence of carbonates in these profiles, previously absent, due to fixation of CO<sub>2</sub>, highlights the potential of these profiles as CO<sub>2</sub> sinks.

## **6. Conclusions**

The profile studied is an example of the complex interaction between groundwater and vadose processes that operate on basaltic-sourced host rocks under arid to semiarid climates. The profile developed on detrital rock

composed of basaltic fragments. In the initial stage (1), alteration of volcanic rock and detrital fragments gave place to the neoformation of red-smectites, and liberated a variety of cations (eg. Mg, K, Na, or Fe) to the interstitial waters. In Stage 2, the initial chabazite precipitation was followed by dolomite formation under phreatic conditions (coarse dolomite). Zoned dolomite indicates changes in water composition, probably due to alternating, always alkaline, drier and wetter conditions. Vadose-pedogenic conditions prevailed in Stage 3 in which dolomicrite formed within the profile. Dominance of calcite at the top of the profile is an indication of the increasing Ca/Mg ratio in the profile, as a result of increasing input of aeolian dust, and decreasing supply of Mg from the hostrock (Stage 4).

Different dolomite textures suggest different formation processes, mostly abiogenic in Stage 2 (coarse zoned dolomite) and biogenic, dominated by roots, in Stages 3 and 4, as indicated by dolomicrite filaments, peloids, and alveolar structures. In both cases, origin of the water was meteoric, as shown by geochemical data, which also confirms the lack of input of deep sourced CO<sub>2</sub>.

Although in volcanic settings, similar profiles have rarely been described, presence of detrital fragments of coarse-zoned dolomite points to reworking of previous profiles, so in these settings these dolocrete profiles may be relatively common. Study of these profiles may clarify the process of transition from a volcanic to a pedogenic environment, and the processes involved in the formation of alkaline surficial paragenesis, containing, for example, carbonates and zeolites.

## Acknowledgements

This work was funded by projects CGL2014-54818-P from the Spanish Ministerio de Ciencia e Innovación. A. Kosir, A. Martín-Pérez and R. Martín-García are thanked for their suggestions during field work. James Cerne reviewed the English version of the manuscript. We thank the reviewers Dr. N. Cabaleri and R. Casillas for their comments to improve the manuscript.

## References

- Alonso-Zarza, A. M., Jones, B., 2007. Root calcrete formation on Quaternary karstic surfaces of Grand Cayman. *Geologica Acta* 5(1), 77-88.
- Alonso-Zarza, A.M., Silva, P.G., 2002. Quaternary laminar calcretes with bee nests: evidences of small-scale climatic fluctuations, Eastern Canary Islands, Spain. *Palaeogeography, Palaeoclimatology, Palaeoecology* 178, 119–135.
- Alonso-Zarza, A.M., Wright, V.P., 2010. Calcretes. In: Alonso-Zarza, A.M., Tanner, L.H. (Eds.), *Developments in Sedimentology. Carbonates in Continental Settings*, Vol. 61. Elsevier, The Netherlands, pp. 225–267.
- Ancochea, E., Barrera, J.L., Bellido, F., Benito, R., Brändle, J.L., Cebriá, J.M., Coello, J., Cubas, C.R., De La Nuez, J., Doblas, M., Gómez, J.A., Hernán, F., Herrera, R., Huertas, J.M., López Ruiz, J., Martí, J., Muñoz, M., Sagredo, J., 2004. Canarias y el Vulcanismo Neógeno peninsular. In: Vera, J.A. (Ed.), *Geología de España*. SGE-IGME, Madrid, 635–682.

- 469 Arakel, A.V., 1986. Evolution of calcrete in palaeodrainages of the Lake  
470 Narpperby area, Central Australia. *Palaeogeography, Palaeoclimatology,*  
471 *Palaeoecology* 54, 283-303.
- 472 Arakel, A.V., 1991. Evolution of Quaternary duricrusts in Karinga Creek  
473 drainage system, central Australian groundwater discharge zone.  
474 *Australian Journal of Earth Sciences* 38, 333-347.
- 475 Ashley, G. M., Driese, S. G., 2000. Paleopedology and paleohydrology of  
476 a volcanoclastic paleosol interval: implications for early Pleistocene  
477 stratigraphy and paleoclimate record, Olduvai Gorge,  
478 Tanzania. *Journal of Sedimentary Research* 70(5), 1065-1080.
- 479 Bajnóczi, B., Kovács-Kis, V., 2006. Origin of pedogenic needle-fiber calcite  
480 revealed by micromorphology and stable isotope composition-a case  
481 study of a Quaternary paleosol from Hungary. *Chemie der Erde* 66, 203-  
482 212.
- 483 Balcells, R., Gómez, J.A., Barrera, J.L., Ruiz, M.T., 2004. Mapa Geológico de  
484 España (1:25.000), 1080 I, IV (Caleta del Sebo). IGME, Madrid.
- 485 Balogh, K., Ahijado, A., Casillas, R., Fernandez, C., 1999. Contributions to the  
486 chronology of the Basal Complex of Fuerteventura, Canary  
487 Islands. *Journal of Volcanology and Geothermal Research* 90, 81-101.
- 488 Brindley, G.W., 1961. Experimental methods. In: Brown, G. (Ed.), *The X-ray*  
489 *Identification and Crystal Structures of Clay Minerals*. Mineralogical  
490 Society, London, 1–50.
- 491 Brown, A. J., Hook, S.J., Baldridge, A.M., Crowley, J.K. Bridges,  
492 N.T., Thomson, B.J., Marion, G.M., de Souza Filho, C.R., Bishop, J.L.,  
493 2010. Hydrothermal formation of clay-carbonate alteration assemblages

- 494 in the Nili Fossae region of Mars, Earth and Planetary Science  
495 Letters, 297, 174-182.
- 496 Bustillo, M. Á., Plet, C., Alonso-Zarza, A. M., 2013. Root calcretes and uranium-  
497 bearing silcretes at sedimentary discontinuities in the miocene of the  
498 Madrid Basin (Toledo, Spain). Journal of Sedimentary Research, 83 (12),  
499 1130-1146.
- 500 Cailleau, G., Verrecchia, E.P., Braissant, O., Emmanuel, L., 2009. The biogenic  
501 origin of needle fibre calcite. Sedimentology 56, 1858–1875.
- 502 Callot, G., Guyon, A., Mousain, D., 1985. Interrelations entre aiguilles de calcite  
503 et hyphes mycéliens. Agronomie 5, 209-216.
- 504 Calvaruso, C., Turpault, M.P., Frey-Klett, P., 2006. Root-associated bacteria  
505 contribute to mineral weathering and to mineral nutrition in trees: A  
506 budgeting analysis. Applied and Environmental Microbiology 72, 1258-  
507 1266.
- 508 Camuera, J., Alonso-Zarza, A.M., Rodríguez-Berriguete, A., Rodríguez-  
509 Gonzalez, A., 2014. Origin and palaeo-environmental significance of the  
510 Berrazales carbonate spring deposit, North of Gran Canaria Island,  
511 Spain. Sedimentary Geology 308, 32- 43.
- 512 Capo, C., Whipkey, C.E., Blachère, J.R., Chadwick, O.A. , 2000. Pedogenic of  
513 dolomite in a basaltic weathering profile, Kohala peninsula,  
514 Hawaii. Geology 28, 271-274
- 515 Carracedo, J.C., 2011. Geología de Canarias I. Origen, evolución, edad y  
516 volcanismo. Rueda S.L. Madrid, 398 pp.
- 517 Carracedo, J.C., Pérez Torrado, F.J., Ancochea, E., Meco, J., Hernán, F.,  
518 Cubas, C.R., Casillas, R., Rodríguez-Badiola, E., Ahijado, A., 2002.

- 519 Cenozoic volcanism II: the Canary Islands. In: W. Gibbons, T. Moreno  
520 (Eds.), *The Geology of Spain*. The Geological Society London, pp. 439–  
521 472.
- 522 Carracedo, J.C., Singer, B., Jicha, B., Guillou, H., Rodríguez Badiola, E., Meco,  
523 J., Pérez-Torrado, F.J., Gimeno, D., Socorro, S., Laínez, A., 2003. La  
524 erupción y el tubo volcánico del Volcán Corona (Lanzarote, Islas  
525 Canarias). *Estudios Geológicos* 59, 277–302.
- 526 Casado, A.I., Alonso-Zarza, A.M., La Iglesia, A., 2014. Morphology and origin of  
527 dolomite in paleosols and lacustrine sequences. Examples from the  
528 Miocene of the Madrid Basin. *Sedimentary Geology* 312, 50-62.
- 529 Chiquet, A., Colin, F., Hamelin, B., Michard, A., Nahon, D., 2000. Chemical  
530 mass balance of calcrete genesis on the Toledo granite (Spain).  
531 *Chemical Geology* 170, 19-35.
- 532 Chiquet, A., Michard, A., Nahon, D., Hamelin, B., 1999. Atmospheric input vs in  
533 situ weathering in the genesis of calcretes: An Sr isotope study at Galvez  
534 (Central Spain). *Geochimica et Cosmochimica Acta* 63, 311-323.
- 535 Coello, J., Cantagrel, J.-M., Hernán, F., Fúster, J.-M., Ibarrola, E., Ancochea,  
536 E., Casquet, C., Jamond, C., Díaz de Téran, J.-R., Cendrero, A., 1992.  
537 Evolution of the eastern volcanic ridge of the Canary Islands based on  
538 new K-Ar data. *Journal of Volcanology and Geothermal Research*, 53(1-  
539 4), 251-274.
- 540 Colson, J., Cojan, I., 1996. Groundwater dolocretes in a lake-marginal  
541 environments: an alternative model for dolomite formation in continental  
542 settings (Danian of the Provence Basin, France). *Sedimentology* 43, 175-  
543 188.

- 544 Criado, C., Torres, J. M., Hansen, A., Lillo, P., Naranjo, A. 2011. Intercalaciones  
545 de polvo sahariano en paleodunas bioclásticas de Fuerteventura (Islas  
546 Canarias). Cuaternario y Geomorfología 26, 73-88.
- 547 Eggleton, R. A., 1984. Formation of iddingsite rims on olivine: A transmission  
548 electron microscope study. Clays and Clay Minerals 32, 1-11.
- 549 Eggleton, R.A., Foudoulis, C., Varkevisser, D., 1987. Weathering of basalt:  
550 changes in rock chemistry and mineralogy. Clay and Clay Minerals, 35,  
551 161-169.
- 552 Esteban, M., Klappa, C., 1983. Subaerial exposure environment. In: Scholle,  
553 P.A., Debout, D.G., Moore, C.H. (Eds). Carbonate Depositional  
554 Environments, Memoir 33, The American Association of Petroleum  
555 Geologists, Oklahoma, USA, 1-54.
- 556 Fúster, J.M., Fernández-Santín, S., Sagredo, J., 1968. Geología y Vulcanología  
557 de las Islas Canarias, Lanzarote. CSIC, Madrid, 177pp.
- 558 Genise, J.F., Alonso-Zarza, A.M., Verde, M., Meléndez, A., 2013. Insect trace  
559 fossils in aeolian deposits and calcretes from the Canary Islands: their  
560 ichnotaxonomy, producers, and palaeoenvironmental significance.  
561 Palaeogeography, Palaeoclimatology, Palaeoecology 377, 110–124.
- 562 Goldsmith, J.R., Graf, D.L., 1958. Structural and compositional variations in  
563 some natural dolomites. The Journal of Geology 66, 678-693.
- 564 Gottardi, G., 1989. The genesis of zeolites. European Journal Mineral 1, 479-  
565 488.
- 566 Goudie, A.S., 1973. Duricrusts in Tropical and Subtropical Landscapes.  
567 Claredon. Oxford, 174 pp.

- 568 Goudie, A.S., Middleton, N.J., 2006. Desert Dust in the Global System.  
569 Springer, Heidelberg. 292 pp.
- 570 Gysi, A.P., Stefánsson, A., 2012. CO<sub>2</sub>-water-basalt interaction. Low  
571 temperature experiments and implications for CO<sub>2</sub> sequestration into  
572 basalts. *Geochimica et Cosmochimica Acta* 81,129-152.
- 573 Hardy, R.,Tucker, M., 1988. X-ray powder diffraction of sediments. In: Tucker,  
574 M.E. (Ed.), *Techniques in Sedimentology*. Blackwell Scientific  
575 Publications, Oxford, 191–228.
- 576 Hay, R. L., Sheppard, R.A., 2001. Occurrence of Zeolites in Sedimentary  
577 Rocks: An Overview. *Reviews in Mineralogy and Geochemistry*, 45, 217-  
578 234.
- 579 Huerta, P., Rodríguez-Berriguete, A., Martín-García, R., Martín-Pérez, A., La  
580 Iglesia, A. Alonso-Zarza, A.M., 2015. The role of climate and eolian dust  
581 input in calcrete formation in volcanic islands (Lanzarote and  
582 Fuerteventura, Spain). *Palaeogeography, Palaeoclimatology,*  
583 *Palaeoecology* 417, 66-79.
- 584 Jutras, P., Utting, J., McLeod, J., 2007. Link between long-lasting evaporitic  
585 basins and the development of thick massive phreatic calcrete hardpans  
586 in the Mississippian Windsor and Percé Groups of eastern Canada.  
587 *Sedimentary Geology* 201, 75-92.
- 588 Kadir, S., Eren, M., Atabey, E., 2010. Dolocretes and associated palygorskite  
589 occurrences in siliciclastic red mudstones of the Sariyer Formation  
590 (Middle Miocene), southeastern side of the Canakkale Strait, Turkey.  
591 *Clay and Clay Minerals*, 58, 205-219.



- 592 Khalaf, F.I., 1990. Occurrence of phreatic dolocrete within Tertiary clastic  
593 deposits of Kuwait, Arabian Gulf. *Sedimentary Geology* 68, 223-239.
- 594 Khalaf, K.F.I., Abdullah, F.A. 2013. Petrography and diagenesis of cavity-fill  
595 dolocretes, *Geoderma* 207–208, 58–65.
- 596 Laurent, B., Marticorena, B., Bergametti, G., Léon, J.F., Mahowald, N.M., 2008.  
597 Modeling mineral dust emissions from the Sahara desert using new  
598 surface properties and soil database. *Journal of Geophysical Research*  
599 113 (D14218).
- 600 Martín-García R., Alonso-Zarza, A.M., Martín-Pérez, A., Schröder-Ritzrau, A.,  
601 Ludwig T., 2014. Relationships between colour and diagenesis in the  
602 aragonite-calcite speleothems in Basajaún Etxea cave, Spain  
603 *Sedimentary Geology* 312, 63-75
- 604 McCrea, J.M., 1950. On the isotope chemistry of carbonates and  
605 paleotemperature scale. *Journal of Chemical Physics* 18, 849–857.
- 606 Meco, J., 2008. *Historia Geológica del clima en Canarias*. International Union of  
607 Geological Sciences. Unesco and ULPGC, Las Palmas de Gran Canaria  
608 296 pp.
- 609 Meléndez, A., Alonso-Zarza, A. M., Sancho, C., 2011. Multi-storey calcrete  
610 profiles developed during the initial stages of the configuration of the  
611 Ebro Basin's exorheic fluvial network. *Geomorphology* 134(3), 232-248.
- 612 Menéndez, I., Díaz-Hernández, J.L., Mangas, J., Alonso, I., Sánchez-Soto, P.J.,  
613 2007. Airborne dust accumulation and soil development in the North-East  
614 sector of Gran Canaria (Canary Islands, Spain). *Journal of Arid*  
615 *Environments* 71 (1), 57–81.

- 616 Ming, D. W., Morris, R. V., Clark, B. C., 2008. Aqueous alteration on Mars. The  
617 Martian Surface—Composition, Mineralogy, and Physical Properties,  
618 519.
- 619 Ming, D.W. and Boettinger, J.L., 2001. Zeolites in Soil Environments. In: Bish,  
620 D.L. y Ming, D.W. (Eds) Natural Zeolites: Occurrence, Properties,  
621 Applications, Reviews in Mineralogy and Geochemistry, Mineralogist  
622 American Society 45, 323-346.
- 623 Muhs, D.R., Budahn, J., Skipp, G., Prospero, J.M., Patterson, D., Bettis Iii, E.A.,  
624 2010. Geochemical and mineralogical evidence for Sahara and Sahel  
625 dust additions to Quaternary soils on Lanzarote, eastern Canary Islands,  
626 Spain. Terra Nova 22 (6), 399–410.
- 627 O'Neil, J. R., Epstein, S., 1966. Oxygen isotope fractionation in the system  
628 dolomite-calcite-carbon dioxide. Science 152 (3719), 198-201.
- 629 Pérez Torrado, F.J., Martí, J., Queralt, I., Mangas, J., 1995. Alteration  
630 processes of the Roque Nublo ignimbrites (Gran Canaria, Canary  
631 Islands). Journal of Volcanology and Geothermal Research 65, 191-204.
- 632 Pérez-Guerrero, D., Buxò, P, Maza, S., Mirabal, R., Ongay, M., Ruiz-Mallén, M.  
633 1997. Depósitos de Zeolitas. In: Melgarejo, J.C (Coord.), Atlas de  
634 asociaciones minerales en lámina delgada. Edicions de la Universitat de  
635 Barcelona, 333-341pp.
- 636 Phillips, S.E., Self, P.G., 1987. Morphology, crystallography and origin of  
637 needle-fibre calcite in Quaternary pedogenic carbonates of South  
638 Australia. Australian Journal Soil Research 25, 429-444.

- 639 Podwojewski, P., 1995. The occurrence and interpretation of carbonate and  
640 sulphate minerals in a sequence of Vertisols in New Caledonia.  
641 *Geoderma* 65, 223-248.
- 642 Robert, C., 2001. Hydrothermal alteration processes of the Tertiary lavas of  
643 Northern Ireland. *Mineralogical magazine* 65(4), 543-557.
- 644 Robert, C., Goffé, B., Saliot, P., 1988. Zeolitization of a basaltic flow in a  
645 continental environment: an example of mass transfer under thermal  
646 control. *Bulletin de minéralogie*, 111(2), 207-223.
- 647 Rodríguez-Berriguete, A., Alonso-Zarza, A.M., Cabrera, M.C., Rodríguez-  
648 Gonzalez, A., 2012. The Azuaje travertine: an example of aragonite  
649 deposition in a recent volcanic setting, N Gran Canaria Island, Spain.  
650 *Sedimentary Geology* 277-278, 61-71.
- 651 Sanz-Montero, M.E., Rodríguez Aranda, J.P., Pérez-Soba, C., 2009. Microbial  
652 weathering of Fe-rich phyllosilicates and formation of pyrite in the  
653 dolomite precipitating environment of a Miocene lacustrine system.  
654 *European Journal Mineralogy* 21, 163-175.
- 655 Sanz-Montero, M.E., Rodríguez-Aranda, J.P., 2012. Endomycorrhizae in  
656 Miocene paleosols: Implications in biotite weathering and accumulation  
657 of dolomite in plant roots (SW Madrid Basin, Spain). *Palaeogeography,*  
658 *Palaeoclimatology, Palaeoecology* 333–334, 121–130
- 659 Scheuvers, D., Schütz, L., Kandler, K., Ebert, M., Weinbruch, S., 2013. Bulk  
660 composition of northern African dust and its source sediments—a  
661 compilation. *Earth-Sciences Reviews* 116, 170–194.

- 662 Spötl, C., Wright, V.P., 1992. Groundwater dolocretes form the Upper Triassic  
663 of the Paris Basin, France: a case study of an arid, continental diagenetic  
664 facies. *Sedimentology* 39, 1119-1136.
- 665 Sutter, B., Boynton W.V., Ming D.W., Niles P.B., Morris, R.V. Golden D.C.,  
666 Lauer, H.V., Fellows, C., Hamara D.K., Mertzman, S.A., 2012. The  
667 detection of carbonate in the Martian soil at the Phoenix Landing site: A  
668 laboratory investigation and comparison with the Thermal and Evolved  
669 Gas Analyzer (TEGA) data. *Icarus* 218, 290–296.
- 670 Van den Bogaard, P., 2013. The origin of the Canary Island Seamount Province-  
671 New ages of old seamounts. *Scientific reports*, 3.
- 672 Verhoef, J., Collette, B. J., Danobeitia, J. J., Roeser, H. A., Roest, W. R., 1991.  
673 Magnetic anomalies off West-Africa (20–38 N). *Marine Geophysical*  
674 *Researches* 13(2), 81-103.
- 675 Verrecchia, E. P., Verrecchia, K. E., 1994. Needle-fiber calcite: a critical review  
676 and a proposed classification. *Journal of Sedimentary Research*, 64(3).  
677 650-664
- 678 Whipkey, Ch.E., Hayob J.L., 2008. Textural and compositional evidence for the  
679 evolution of pedogenic calcite and dolomite in a weathering profile on the  
680 Kohala Peninsula, Hawaii. *Carbonates and Evaporite* 23, 104-112.
- 681 Whipkey,, Ch.E., Capo, R.C., Hsieh, J. C.C., Chadwick, O.A., 2002.  
682 Development of Magnesian Carbonates in Quaternary Soils on the Island  
683 of Hawaii. *Journal of Sedimentary Research* 72, 158-165.
- 684 Williams, C.A., Krause, F.F., 1998. Pedogenic-phreatic carbonates on a Middle  
685 Devonian (Givetian) terrigenous alluvial-deltaic plain, Gilwood Member

686 (Watt Mountain Formation), northcentral Alberta, Canada. *Sedimentology*  
687 45, 1105-1124.

688 Wilson, M.J., 1999. The origin and formation of clay minerals in soils: past,  
689 present and future perspectives. *Clay Minerals* 34, 7-25.

690 Wright, V. P., Barnett, A. J., 2015,. An abiotic model for the development of  
691 textures in some South Atlantic early Cretaceous lacustrine  
692 carbonates. *Geological Society, London, Special Publications*, 418,  
693 SP418-3.

694 Yanes, Y., Delgado, A., Castillo, C., Alonso, M.R., Ibáñez, M., De la Nuez, J.,  
695 Kowalewski, M., 2008. Stable isotope ( $\delta^{18}\text{O}$ ,  $\delta^{13}\text{C}$ , and  $\delta\text{D}$ ) signatures  
696 of recent terrestrial communities from a low-latitude, oceanic Setting:  
697 endemic land snails, plants, rain, and carbonate sediments from the  
698 eastern Canary Islands. *Chemical Geology* 249, 377-392.

699 Zazo, C., Goy, J. L., Hillaire-Marcel, C., Gillot, P. Y., Soler, V., González, J. Á.,  
700 Dabrio, J.C. Ghaleb, B., 2002. Raised marine sequences of Lanzarote  
701 and Fuerteventura revisited—a reappraisal of relative sea-level changes  
702 and vertical movements in the eastern Canary Islands during the  
703 Quaternary. *Quaternary Science Reviews* 21(18), 2019-2046.

704

705

706

## FIGURE CAPTIONS

Table 1. Mineralogy and isotope data of the studied samples.

Fig. 1. Map showing the location of the Mirador del Río profile and the geology of the studied area. 1. Hierro, 2. La Palma, 3. Gomera, 4. Tenerife, 5. Gran Canaria, 6. Fuerteventura, 7. Lanzarote.

Fig. 2. Sedimentary log of the Mirador del Río profile and its mineralogy.

Fig. 3. (A) Outcrop of the Mirador del Río profile with indication of the three horizons: lower (L), intermediate (I) and upper (U). (B) Intermediate horizon in which the red cracked sandy mudstones (1) include white carbonate layers (2). (C) Closed-up view of the sandy mudstones with cracks filled partially by chabazite and dolomite cements (arrowed).

Fig. 4. Microphotographs of thin sections: (A) Sandy mudstones of the intermediate horizon composed by a dolomicrite groundmass (g) with volcanic fragments (v) and cracks (arrowed) filled with dolomite (d) and chabazite. (B) The dolomicrite groundmass of the dolomite layers of the intermediate horizon also includes large volcanic fragments (v) and detrital dolomite grains (arrowed, d). (C) Calcitic layers consist of a micrite groundmass with volcanic fragments (v) coated by micrite (arrowed) and locally laminated micrite (arrowed).

Fig. 5. Sketches of the micromorphology of the different parts of the profile. A. Intermediate horizon, cracked sandy mudstones. B. Intermediate horizon dolomitic layers. C. Upper horizon.

Fig. 6. (A) Coarse altered and broken olivine fragment (ol). (B) Detrital grain with a thin clay coating (arrowed). (C) Detailed view of a clay coating showing

an open structure characteristic of smectites (arrowed). (D). Fibrous-radial chabazite (ch) filling cracks within the groundmass, coarse zoned dolomite grew in the remaining porosity. (E, F). Same image under parallel and crossed nichols showing chabazite (ch), coarse zoned dolomite (d) and dolomicrite groundmass (dm).(G, H) The infill of the porosity of the mudstone layers is made by spheroidal chabazite and coarse zoned dolomite which partially replaces chabazite.

Fig. 7. Carbonate layers. (A) Chabazite and coarse zoned dolomite filling cracks within the dolomicrite groundmass. (B) Detrital fragments of coarse zoned dolomite. (C) Peloidal dolomicrite groundmass containing detrital fragments some composed of dolomite (d) and chabazite (ch). (D) Dolomicrite containing some detrital grains coated by dolomicrite (arrowed). (E) Organic filaments within the dolomicrite groundmass. (F) Needle crystals within the dolomicrite. (G) Micritic filaments (arrowed) and peloids (arrowed) filling partially a crack within the calcite groundmass. (H) Alveolar septal structures in the topmost horizon.

Fig. 8.  $\delta^{13}\text{C}$  ‰VPDV and  $\delta^{18}\text{O}$  ‰VPDV plots of the carbonates of the Mirador del Río profile and comparison with other calcretes from Lanzarote and Fuerteventura (Huerta et al., 2015).

Fig. 9. Model illustrating the 4 stages of development of Mirador del Río profile. For legend see Fig. 2.

Figure 1  
[Click here to download high resolution image](#)

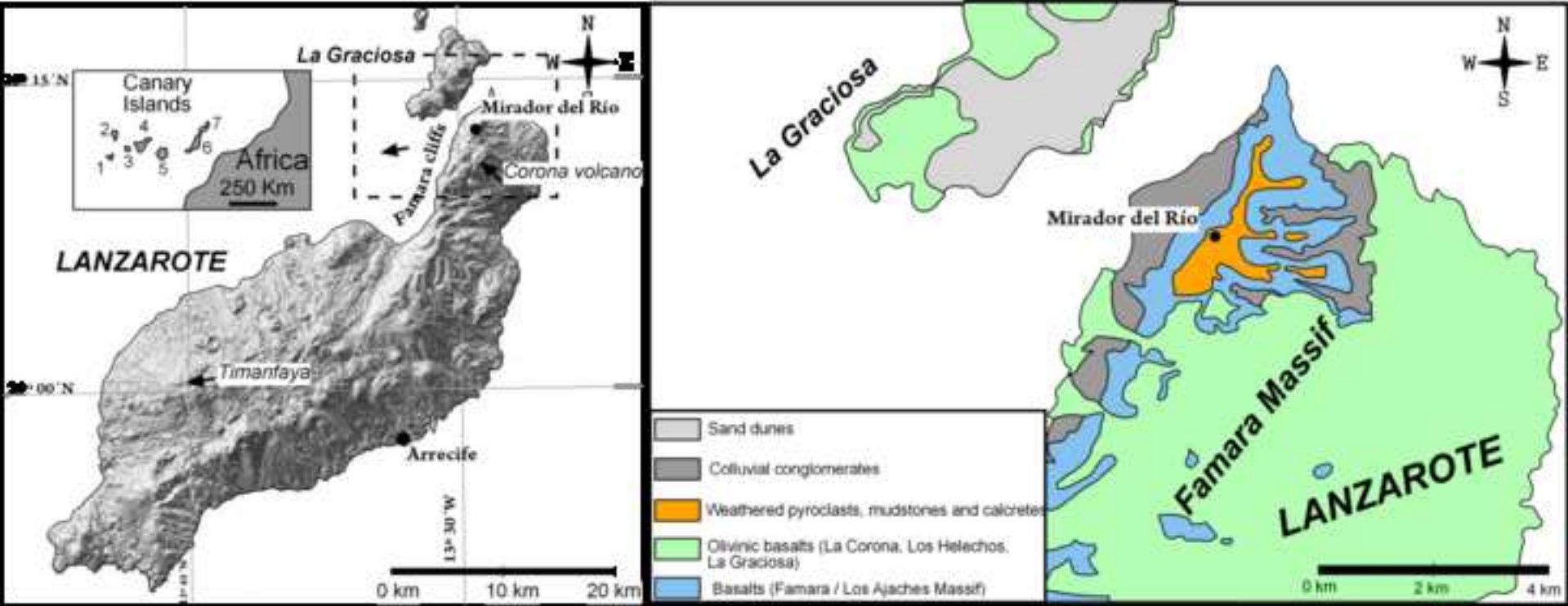




Figure 2  
[Click here to download high resolution image](#)

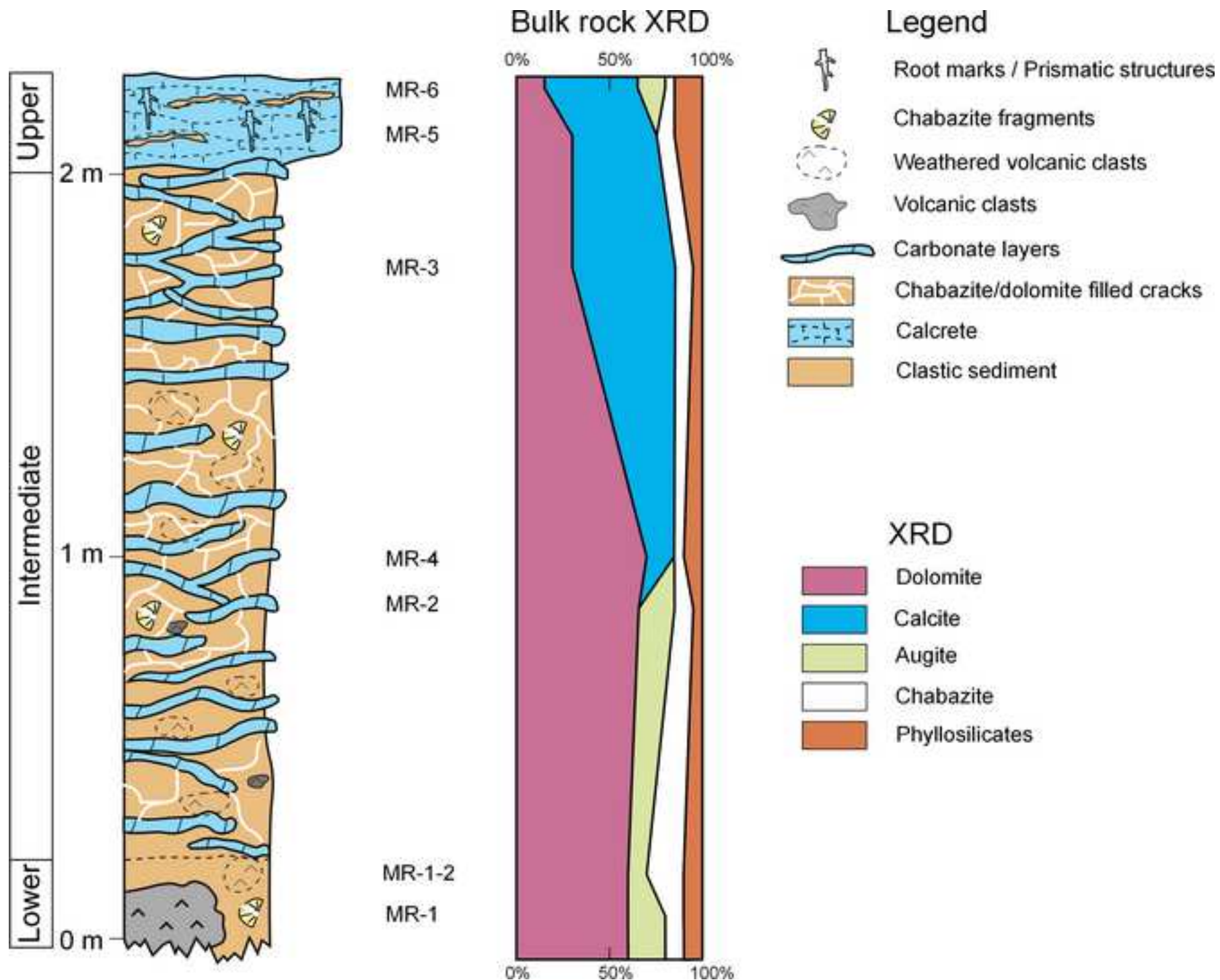


Figure 3  
[Click here to download high resolution image](#)

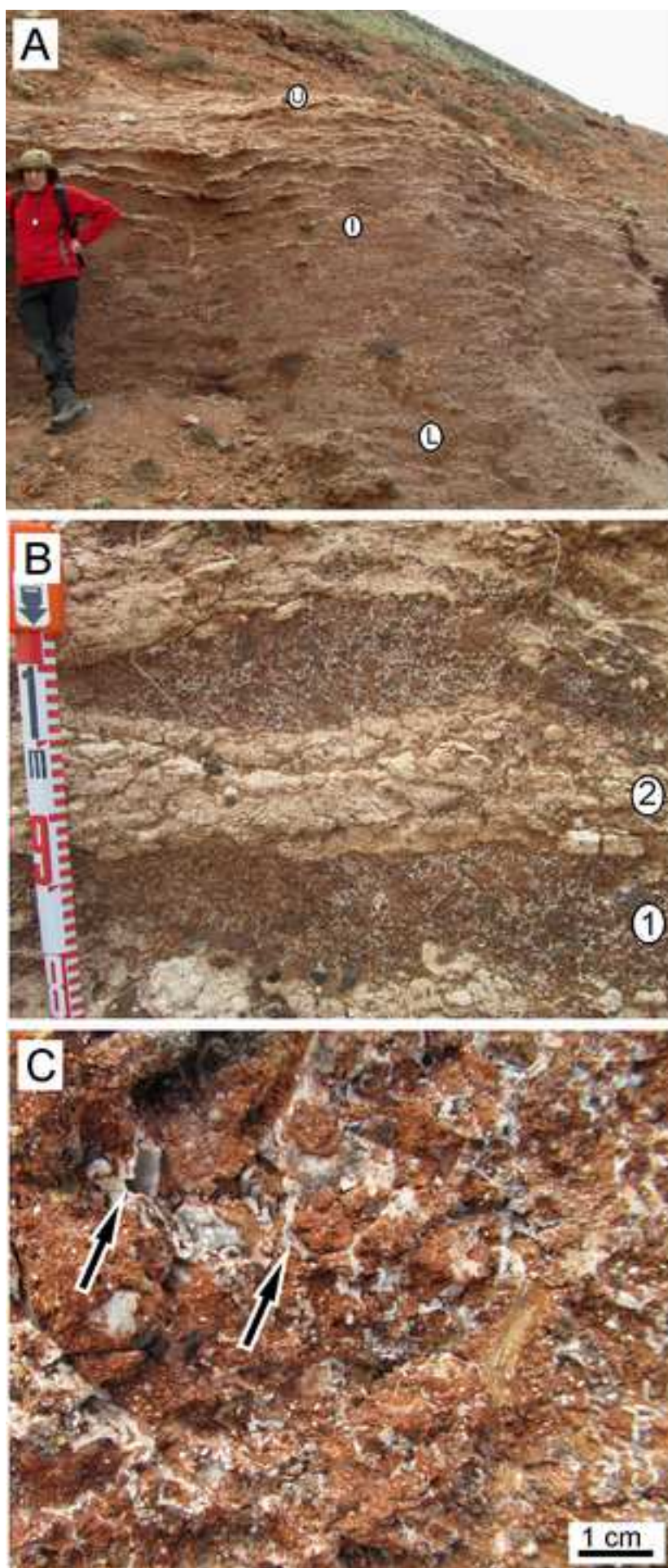




Figure 4  
[Click here to download high resolution image](#)

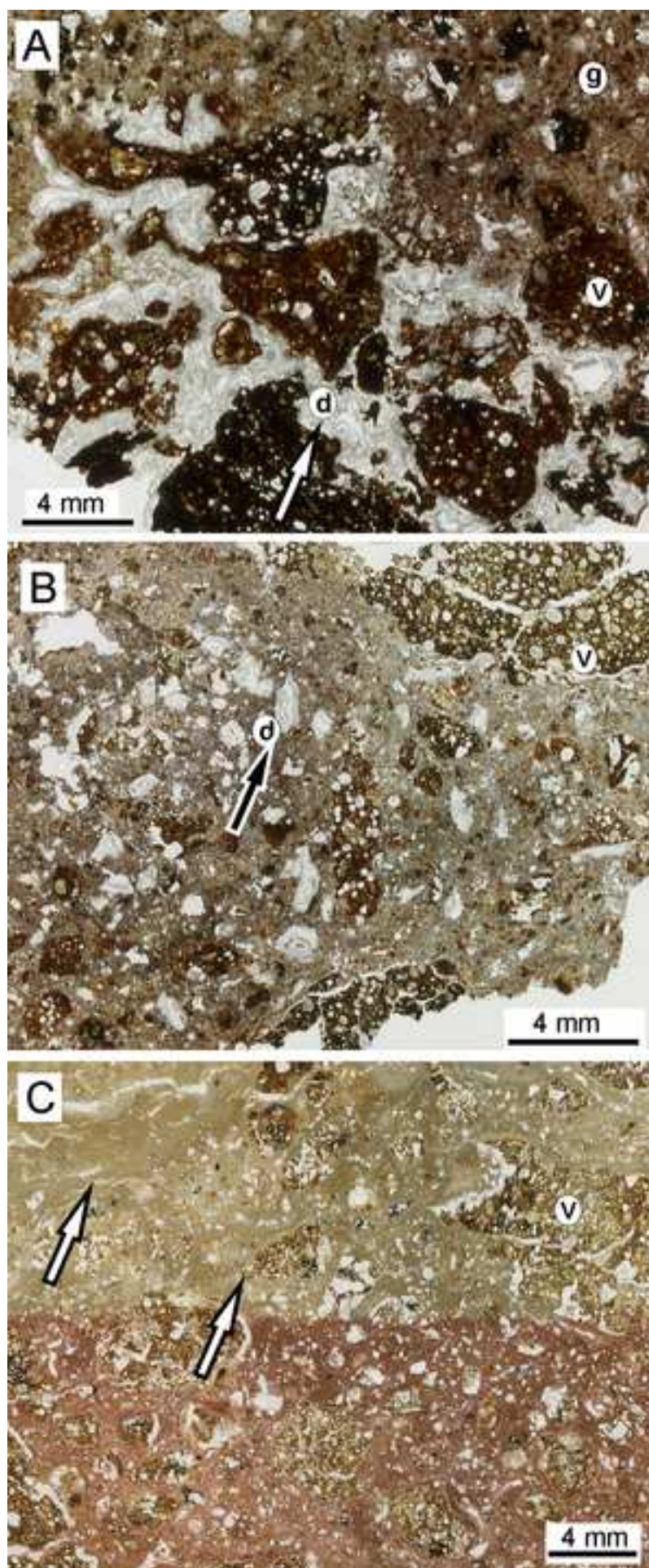
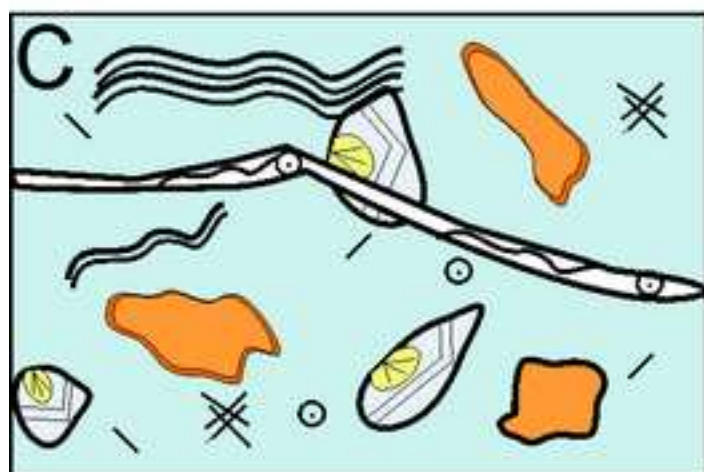
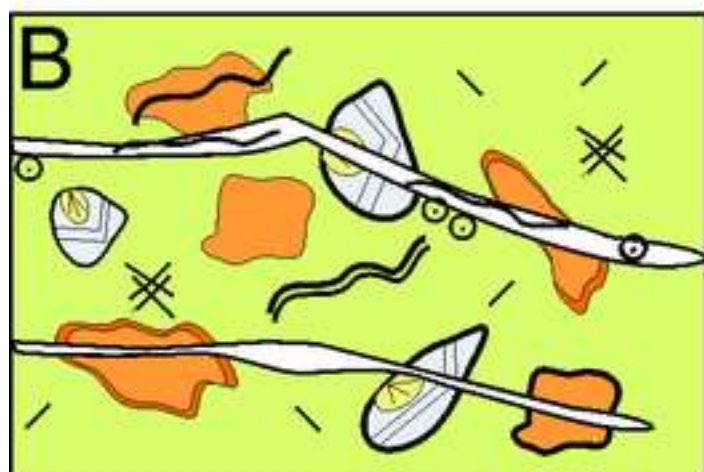
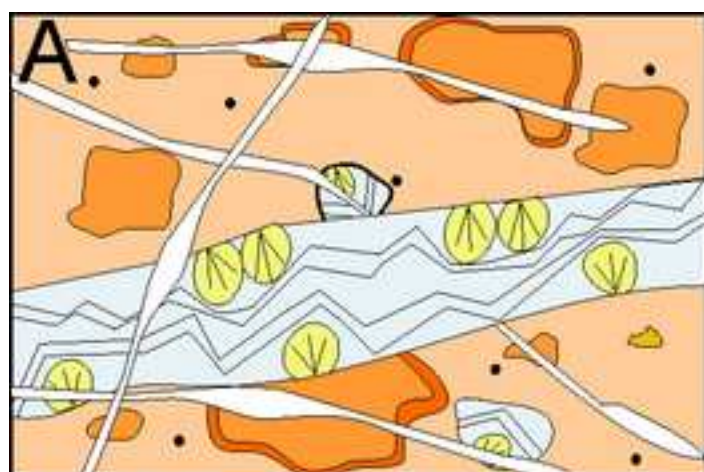


Figure 5  
[Click here to download high resolution image](#)




-  Dolomite
-  Calcite
-  Sandy mudstone
-  Micrite
-  Clays
-  Zoned dolomite
-  Chabazite
-  Crack
-  Micrite filament
-  Volcanic fragment
-  Clay coating
-  Micrite coating
-  Peloid/coated grain
-  Needle fibre crystals
-  Laminar structure
-  Chabazite + dolomite fragment



Figure 6  
[Click here to download high resolution image](#)

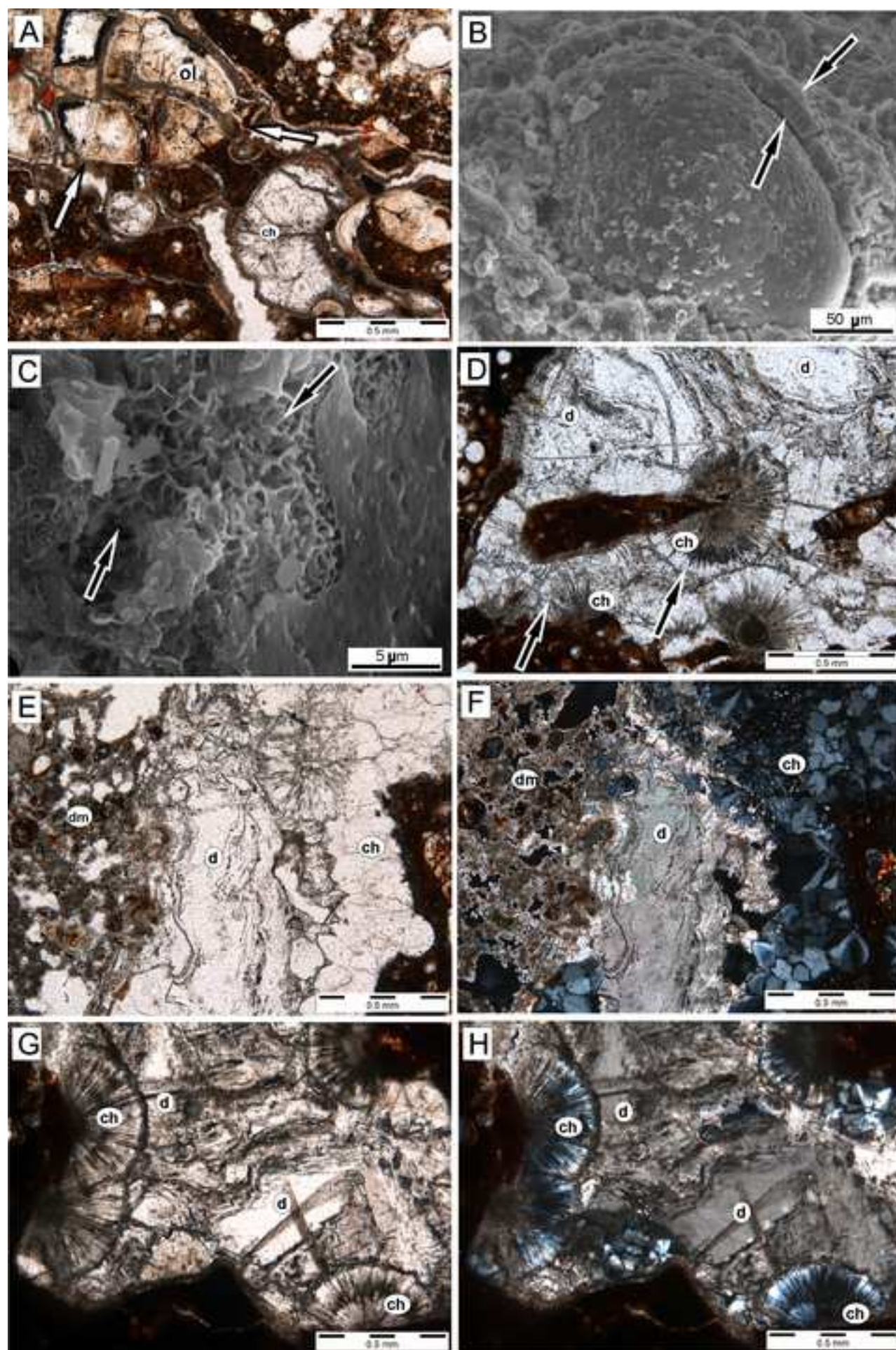




Figure 7  
[Click here to download high resolution image](#)

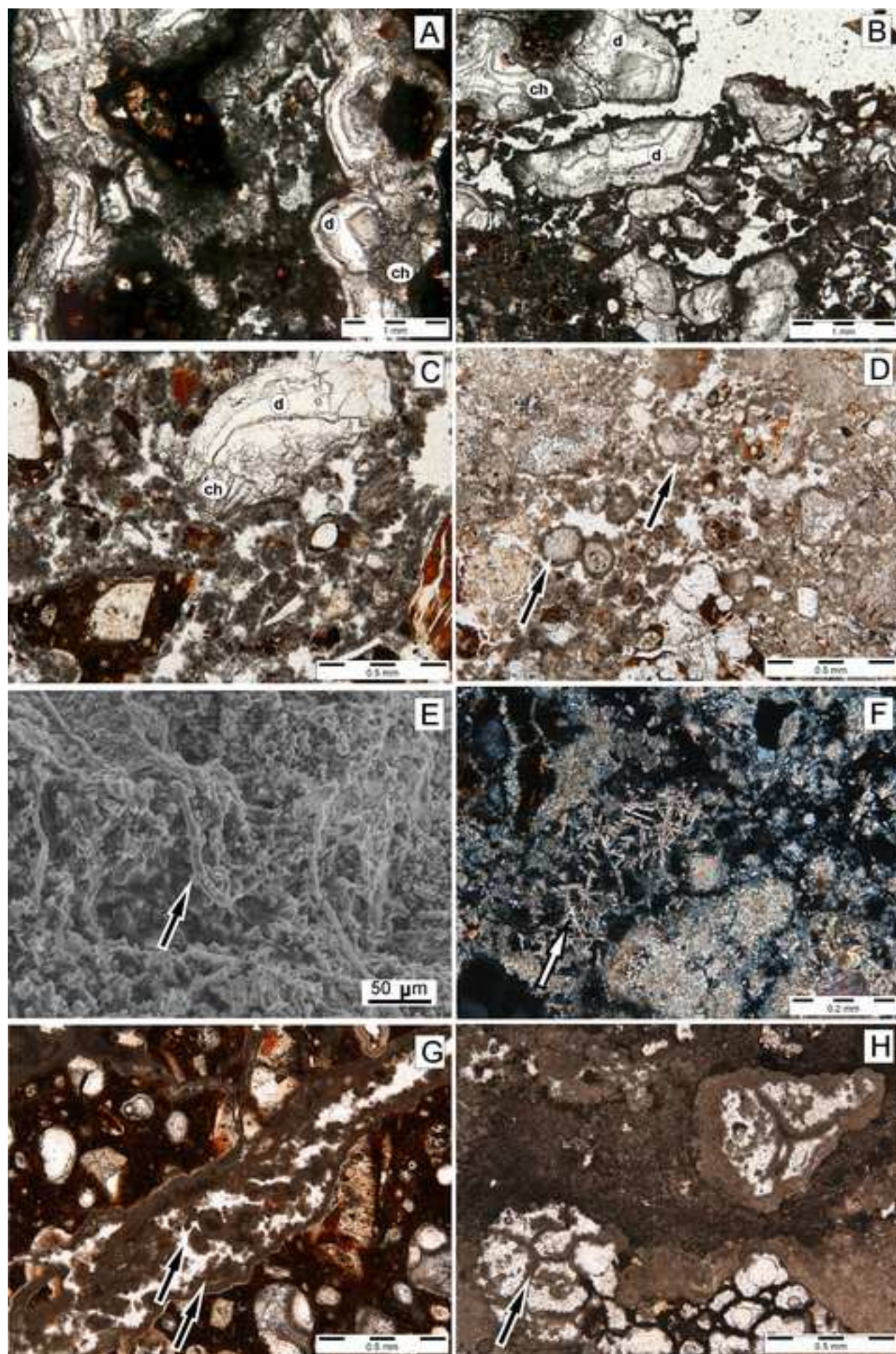


Figure 8

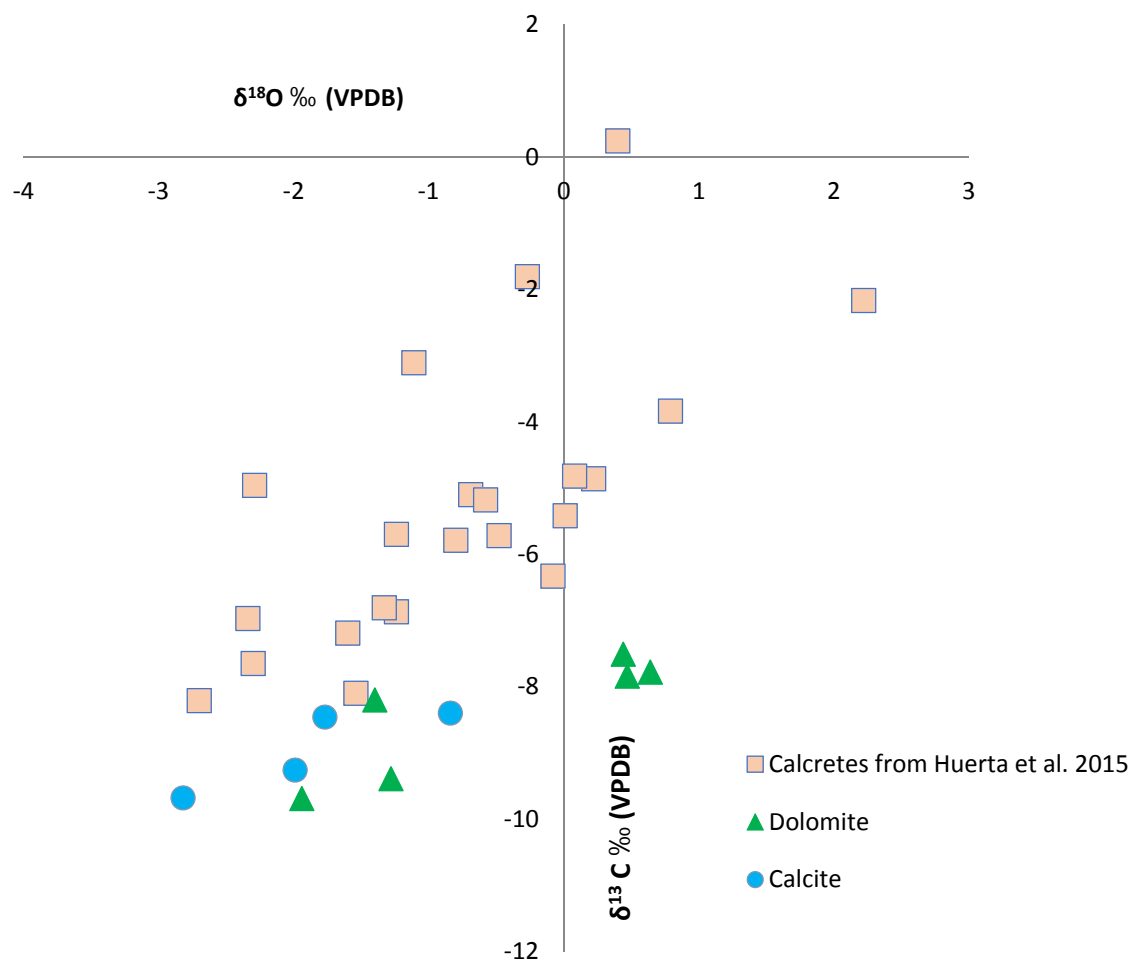




Figure 9  
[Click here to download high resolution image](#)

